Supplement of Geosci. Model Dev., 15, 5489–5510, 2022
https://doi.org/10.5194/gmd-15-5489-2022-supplement

Geoscientific Model Development
Open Access
EGU

Supplement of

Spatial heterogeneity effects on land surface modeling of water and energy partitioning

Lingcheng Li et al.

Correspondence to: Lingcheng Li (lingcheng.li@pnnl.gov)

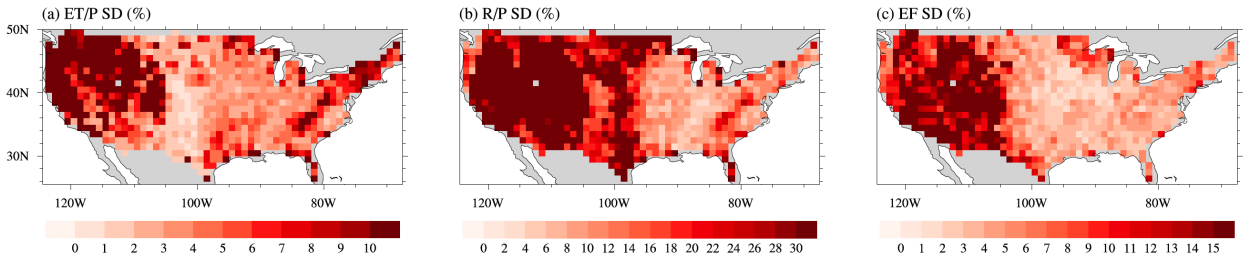

Figure S1. The normalized standard deviation (SD) range of 16 experiments for the annual climatology of (a) ET/P, (b) R/P, and (c) EF. For a given variable (e.g., ET/P), The range of SD is calculated as the difference between the maximum and minimum (i.e., 0 of the experiment A0S0L0T0) SD of these 16 experiments. The climatological mean from experiment A0S0L0T0 is used to normalize the SD, the ratio between SD and mean, to obtain normalized SD. The normalized SD represents how large the heterogeneity affects the spatial variability of a given variable compared to its climatological mean.

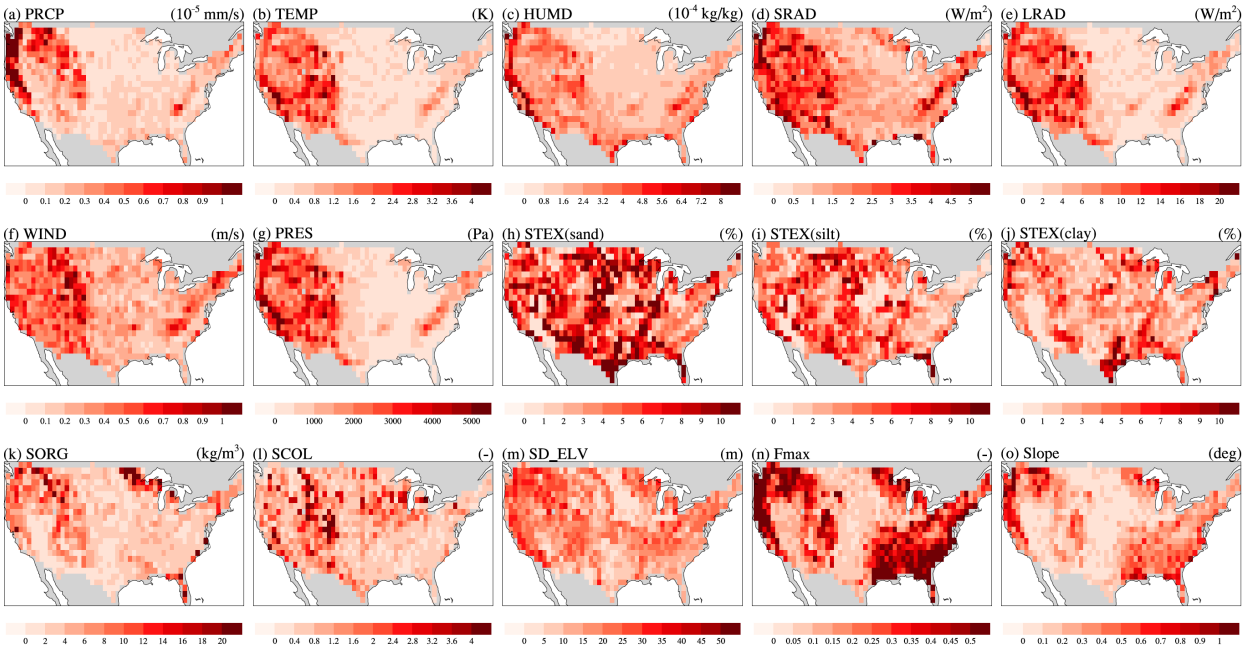

Figure S2 Spatial variability (i.e., SD) of each component of three heterogeneity sources. SD is calculated at each 1°×1° region based on 0.125° data. ATM: the annual climatological mean of (a) precipitation, (b) temperature, (c) humidity, (d) shortwave radiation, (e) longwave radiation, (f) wind speed, and (g) air pressure. SOIL: (h) percentage of sand at surface five soil layers, (i) percentage of silt at surface five soil layers, (j) percentage of clay at surface five soil layers, (k) soil organic matter at surface five soil layers, (l) soil color. TOPO: (m) standard deviation of elevation, (n) Fmax, (o) slope.

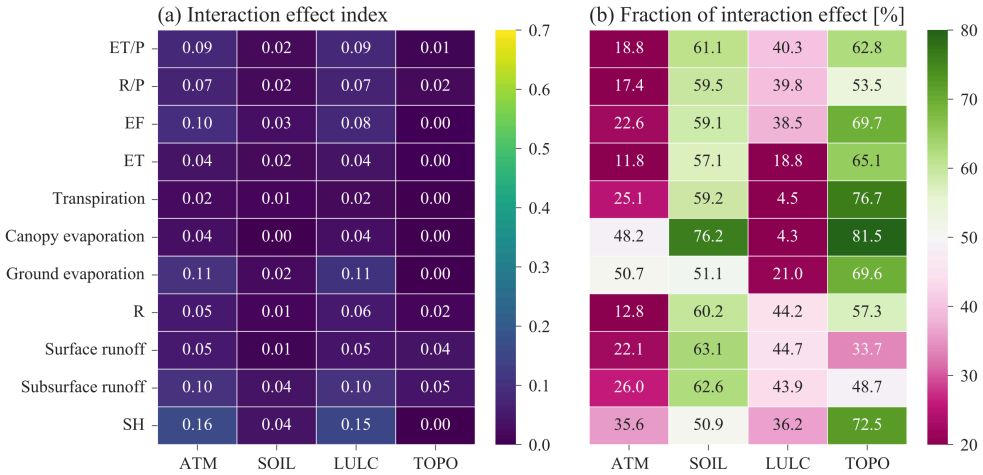

Figure S3. CONUS averaged Sobol' (a) interaction effect index, SI_{X_i}, and (c) fraction of interaction effect, $f_{SI_{X_i}}$, for the sensitivity of spatial variability of different variables (rows) to the four heterogeneity sources (columns).

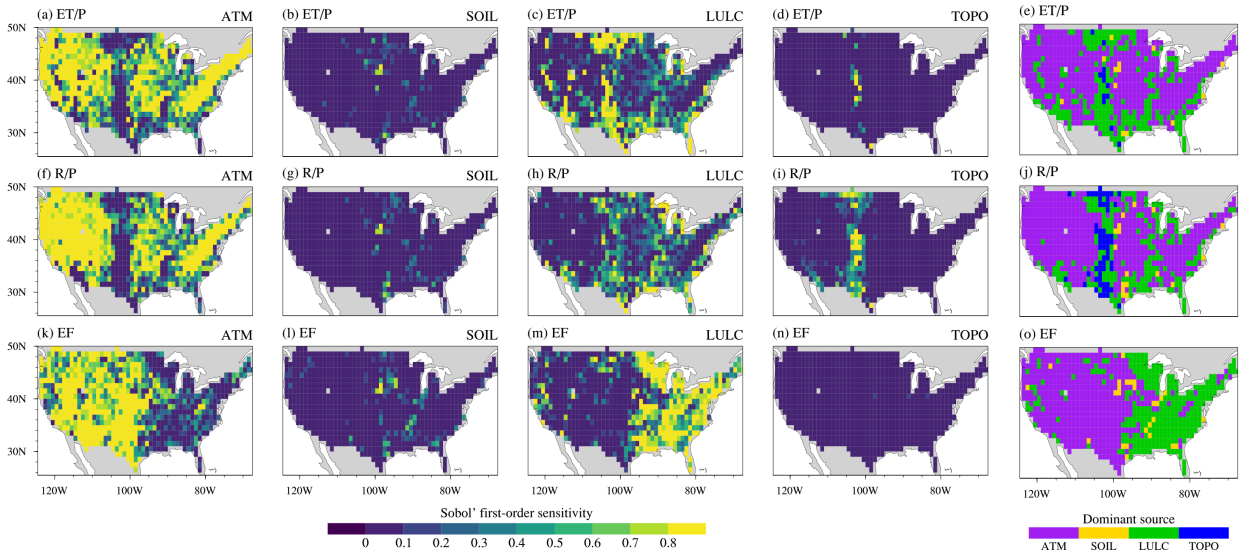

Figure S4. Same as Figure 4 in the main text, but for Sobol' first-order sensitivity index. Spatial patterns of Sobol' first-order sensitivity index for the four heterogeneity sources (column 1-4) and the corresponding dominant sources (column 5) for the spatial variability of water (ET/P and R/P) and energy (EF) partitioning.

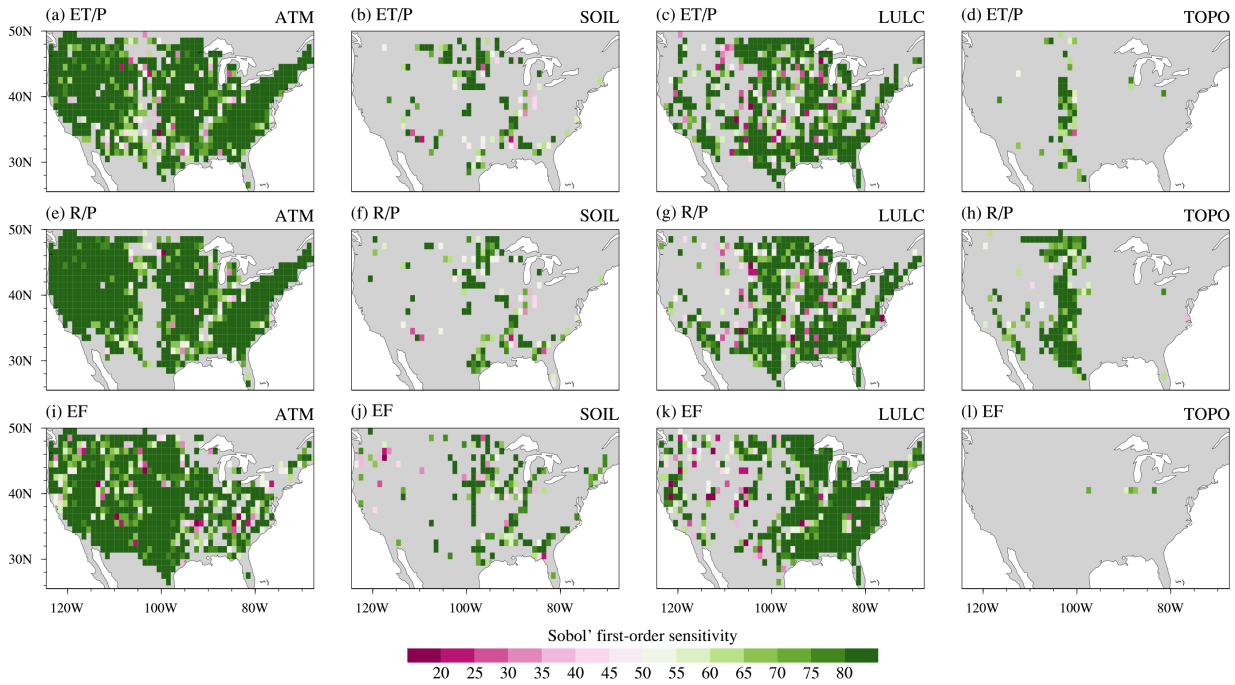

Figure S5. Spatial patterns of the first-order sensitivity index fraction for the four heterogeneity sources. Only grids with Sobol' total sensitivity index larger than 0.05 are shown. The green color means the first-order sensitivity index mainly contributes to Sobol' total sensitivity.

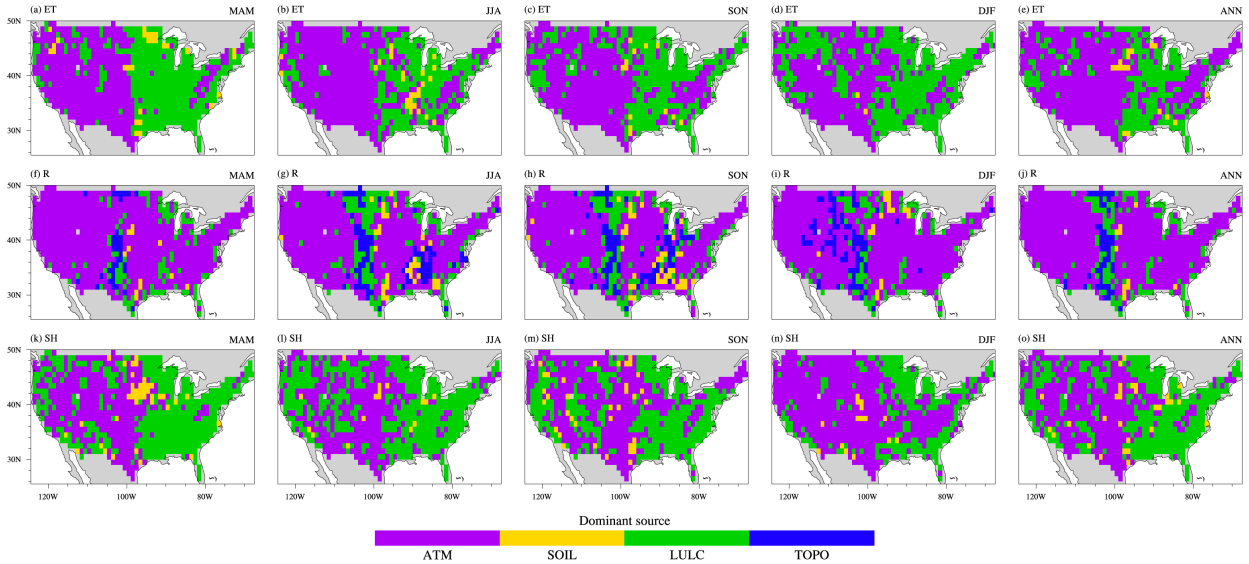

Figure S6. Spatial patterns of the most sensitive heterogeneity source for ET, R, and SH in four seasons and annual mean.

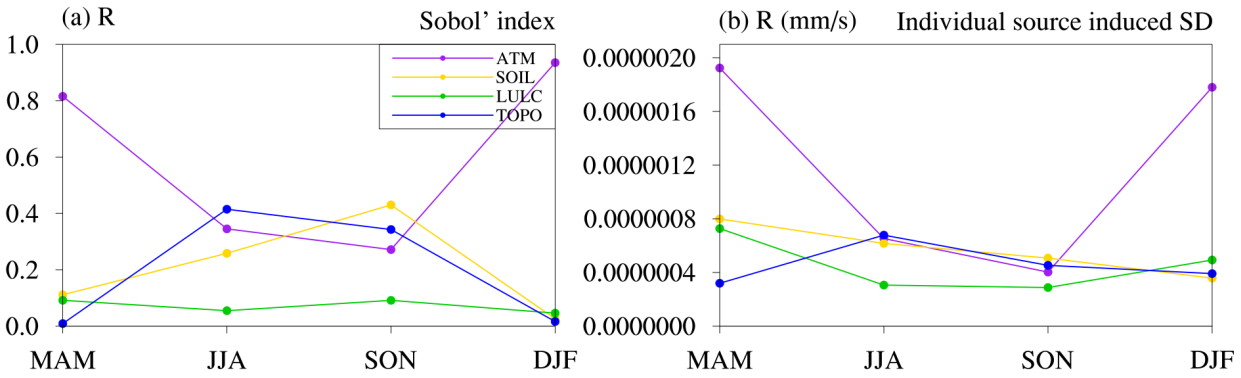

Figure S7 Demonstration of the seasonal variations of (a) Sobol' total sensitivity index and (b) individual source induced SD for four heterogeneity sources at the one eastern US grid (latitude: 32.5° N, longitude: 86.5° W). Following Appendix B in the main text, EXP9, EXP5, EXP3, and EXP2 roughly represent the sole heterogeneous effect from ATM, SOIL, LULC, and TOPO, respectively. The R's SD in (b) is computed from the seasonal climatology of each experiment (see section 2.3 in the main text), roughly representing the sole heterogeneity effect from each source.

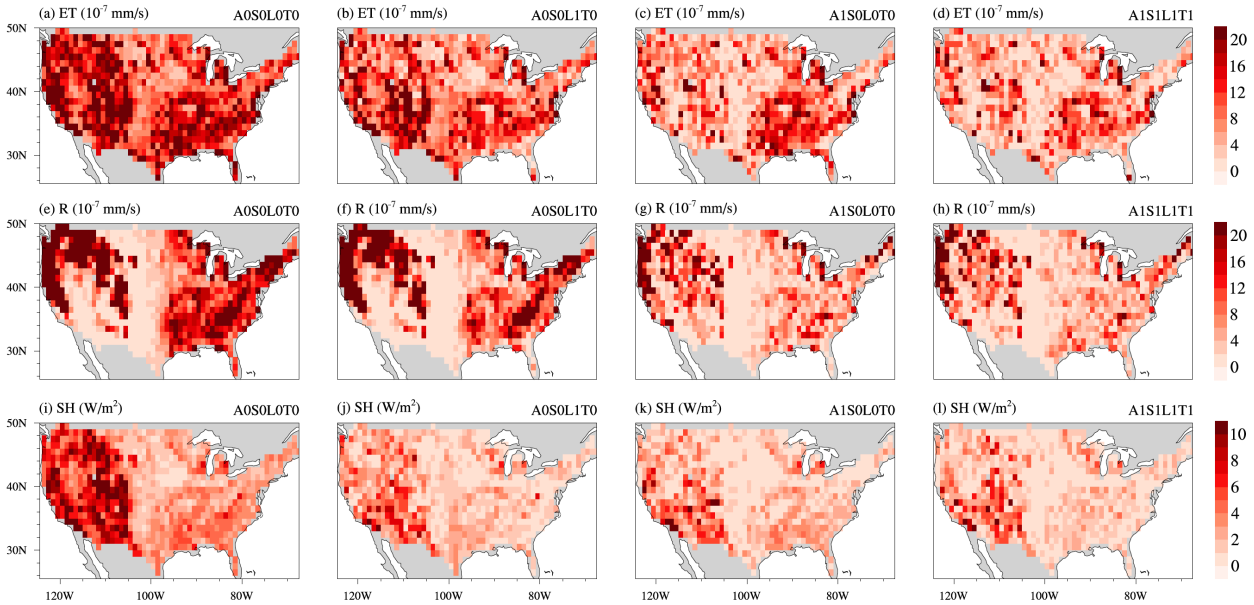

Figure S8. CONUS spatial patterns of SD's absolute difference between four ELM experiments and ERA5-Land reanalysis for the annual climatological mean of ET (top panel), R (middle panel), and SH (bottom panel). 1st column figures represent the homogeneous experiment (A0S0L0T0); 2nd column figures show only LULC effects based on EXP3 (A0S0L1T0); 3rd column figures represent only ATM effects based on EXP3 (A0S0L1T0); 4th column figures represent effects from all four heterogeneity sources based on EXP16 (A1S1L1T1).

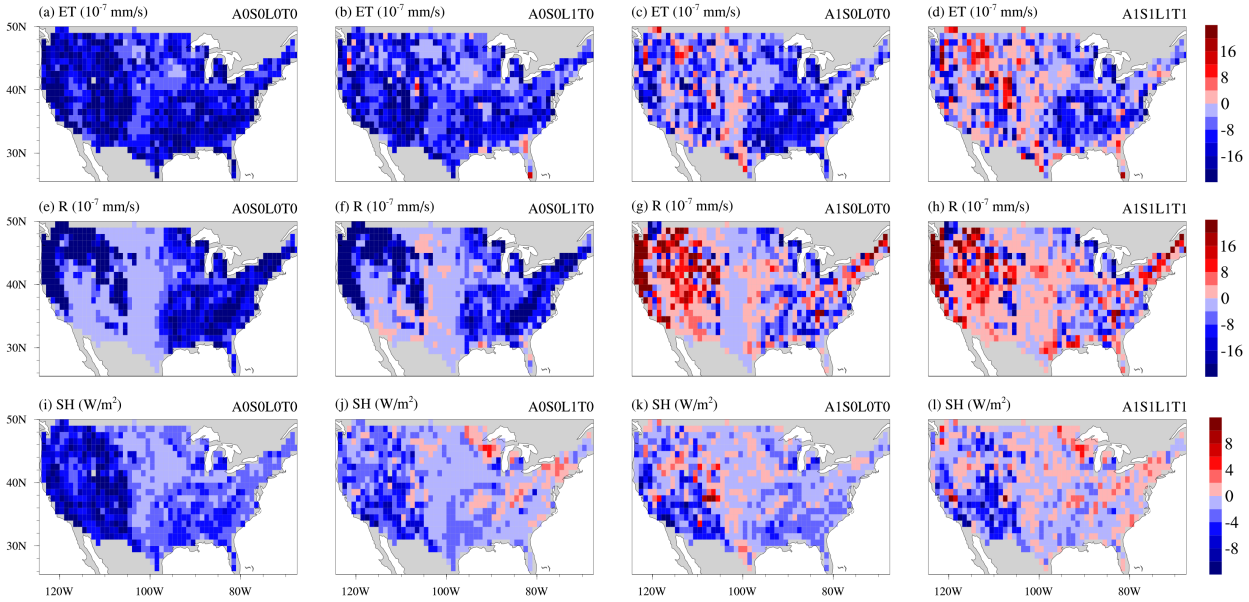

Figure S9. Similar to Figure S8 but for the SD's difference between four ELM experiments and ERA5-Land reanalysis (i.e., ELM – ERA5_Land).